Technical Notes

TECHNICAL NOTES are short manuscripts describing new developments or important results of a preliminary nature. These Notes cannot exceed 6 manuscript pages and 3 figures; a page of text may be substituted for a figure and vice versa. After informal review by the editors, they may be published within a few months of the data of receipt. Style requirements are the same as for regular contributions (see inside back cover).

A New Momentum Integral Method for MHD Channel Entrance Flows

R. E. SCHWIRIAN*
NASA Lewis Research Center, Cleveland, Ohio

Nomenclature

a = channel half-width (Y direction)
B = magnetic field strength
C_f = local friction coefficient
$\langle C_f \rangle$ = average friction coefficient
C_{fB} = Blasius friction coefficient = $0.664\ (\mu/\rho U X)^{1/2}$
E = electric field strength
f = "edge" stress function
K = load parameter = $E/\langle U \rangle B$
M = Hartmann number = $Ba(\sigma/\mu)^{1/2}$
p = pressure
P_L = nondimensional pressure drop = $(p - p_0)/\rho\langle U \rangle^2$
Re = Reynolds number = $4\rho\langle U\rangle a/\mu$
U = freestream velocity
$\langle U \rangle$ = average velocity
u = velocity in boundary layer
u^* = dimensionless velocity = $u/\langle U \rangle$
X = coordinate parallel to flow
x = X/a
x_1 = $4x/Re$
x_2 = $4M^2x/Re$
Y = coordinate parallel to magnetic field
y = Y/a
Z = coordinate perpendicular to X and Y
α_L = see Eq. (4)
δ = boundary-layer thickness
δ^* = displacement thickness
ϵ = δ/a
ϵ^* = ϵ/ϵ_∞
η = Y/δ
θ = momentum thickness
μ = viscosity
ρ = mass density
σ = electrical conductivity
τ_e = "edge" stress
τ_w = wall stress

Subscripts

L = laminar
w = wall
o = entrance value
∞ = asymptotic value

A MOMENTUM integral technique has been developed which[1] uses a boundary-layer "edge" shear stress τ_e to derive core flow and boundary-layer equations of motion for magnetohydrodynamic (MHD) entrance flows. The edge stress acts as a viscous coupling between the boundary layer and the core flow and allows the latter to develop a viscous pressure drop, which standard momentum integral techniques[2-6] do not permit. Basically, the governing equations are integral forms of Prandtl's boundary-layer equations with a shear stress τ_e acting between the boundary-layer and core flow. By defining an edge stress function $f(\epsilon)$ such that

$$\tau_e/(1 - \epsilon) = \tau_w f(\epsilon) \tag{1}$$

and using a parabolic velocity profile for laminar flow, the nondimensionalized equation of motion becomes

$$\left[\frac{2 + \frac{7}{3}\epsilon}{(1 - \epsilon/3)^2}\right]\frac{d(\epsilon^*)^2}{dx} = \frac{120}{Re}\left[\frac{2(1 - f)}{\epsilon_\infty{}^2} - \frac{M^2}{3}(\epsilon^*)^2\right] \tag{2}$$

The values of ϵ_∞ and $f(\epsilon_\infty) \equiv f_\infty$ are obtained by requiring that 1) the asymptotic wall stress as computed from the boundary-layer profile be equal to the exact Hartmann flow value[7] and 2) Eq. (2) yield solutions which are asymptotic to ϵ_∞. The entrance values ϵ_0 and $f(\epsilon_0) \equiv f_0$ depend on the initial conditions. Two entrance velocity profiles of particular interest are 1) the uniform velocity profile and 2) the fully developed nonmagnetic Poiseuille flow profile.[5] Although both of these cases can be treated with the present method,[1] results will be presented only for the first, since it has been extensively treated in the literature.

For values of ϵ between ϵ_0 and ϵ_∞ the quantity $\tau_e/(1 - \epsilon)$ is taken to vary as a linear combination of the two perturbing forces in such a way that the function f passes through its initial and final values. These perturbing forces are the wall stress τ_w, which is inversely proportional to the boundary-layer thickness and the Lorentz force term, which is directly proportional to the boundary-layer thickness. Equation (2) then becomes

$$[2 + \tfrac{7}{3}\epsilon/(1 - \epsilon/3)^2]d(\epsilon^*)^2/dx = \alpha_L(1 - \epsilon^{*2}) \tag{3}$$

where

$$\alpha_L = \frac{120}{Re}\left[\frac{2(1 - f_0)/\epsilon_\infty{}^2 - (M^2/3)\epsilon_0{}^{*2}}{1 - \epsilon_0{}^{*2}}\right] \tag{4}$$

This equation can be integrated by partial fractions to yield

$$x = \frac{18}{\epsilon_\infty{}^2\alpha_L}\left\{\phi_1 \ln\left(\frac{\epsilon^* - 1}{\epsilon_0{}^* - 1}\right) + \phi_2 \ln\left(\frac{\epsilon^* + 1}{\epsilon_0{}^* + 1}\right) + \phi_3 \ln\left(\frac{\epsilon^* - 3/\epsilon_\infty}{\epsilon_0{}^* - 3/\epsilon_\infty}\right) - \phi_4[(\epsilon^* - 3/\epsilon_\infty)^{-1} - (\epsilon_0{}^* - 3/\epsilon_\infty)^{-1}]\right\} \tag{5}$$

where

$$\phi_1 = -(2 + \tfrac{7}{3}\epsilon_\infty)/2(3/\epsilon_\infty - 1)^2$$

$$\phi_2 = -(2 - \tfrac{7}{3}\epsilon_\infty)/2(3/\epsilon_\infty + 1)^2$$

$$\phi_3 = -(\phi_1 + \phi_2); \quad \phi_4 = 27/\epsilon_\infty(1 - 9/\epsilon_\infty{}^2)$$

An approximation to Eq. (5), valid when $\epsilon \ll 1$ for all values of X, is

$$\epsilon^* = [1 + (\epsilon_0{}^{*2} - 1)\exp(-\alpha_L x/2)]^{1/2} \tag{6}$$

The local and average friction coefficients C_{fL} and $\langle C_{fL}\rangle$ and the nondimensional pressure drop P_L are given by

$$C_{fL} = \frac{2\tau_w}{\rho\langle U\rangle^2} = \frac{16}{\mathrm{Re}(1 - \epsilon_\infty\epsilon^*/3)\epsilon_\infty\epsilon^*} \tag{7}$$

Presented as Paper 69-724 at the AIAA Fluid and Plasma Dynamics Conference, San Francisco, Calif., June 16–18, 1969; submitted June 9, 1969; revision received October 29, 1969.

* Aerospace Engineer, Plasma Power Generation Section, Electromagnetic Propulsion Division. Member AIAA.

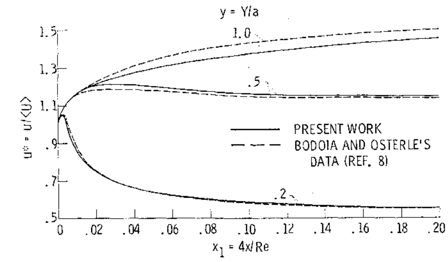

Fig. 1 Laminar flow velocity development for zero Hartmann number.

$$\langle C_{fL}\rangle = \frac{864}{\epsilon_\infty{}^4\alpha_L}\left(\frac{1}{Rex}\right)\left\{-\psi_1\ln\left(\frac{\epsilon^*-1}{\epsilon_0{}^*-1}\right)+\psi_2\ln\left(\frac{1+\epsilon^*}{1+\epsilon_0{}^*}\right)-\psi_3\ln\left(\frac{\epsilon^*-3/\epsilon_\infty}{\epsilon_0{}^*-3/\epsilon_\infty}\right)-\psi_4\left[\left(\epsilon^*-\frac{3}{\epsilon_\infty}\right)^{-1}-\left(\epsilon_0{}^*-\frac{3}{\epsilon_\infty}\right)^{-1}\right]+\frac{\psi_5}{2}\left[\left(\epsilon^*-\frac{3}{\epsilon_\infty}\right)^{-2}-\left(\epsilon_0{}^*-\frac{3}{\epsilon_\infty}\right)^{-2}\right]\right\} \quad (8)$$

$$P_L = \frac{p-p_0}{\rho\langle U\rangle^2} = -\frac{x}{2}\langle C_{fL}\rangle - \frac{4M^2}{Re}x(1-K) + \frac{(1-\frac{7}{15}\epsilon_0)}{(1-\epsilon_0/3)^2} - \frac{(1-\frac{7}{15}\epsilon_\infty\epsilon^*)}{(1-\epsilon_\infty\epsilon^*/3)^2} \quad (9)$$

where

$$\psi_1 = -\phi_1/(3/\epsilon_\infty - 1);\quad \psi_2 = -\phi_2/(3/\epsilon_\infty + 1)$$
$$\psi_3 = \psi_2 - \psi_1$$
$$\psi_4 = (1 - 9/\epsilon_\infty)\psi_1 + (1 + 9/\epsilon_\infty)\psi_2 - 6/\epsilon_\infty\psi_3$$
$$\psi_5 = 9/(1 - 9/\epsilon_\infty{}^2)$$

Discussion of Results

Figure 1 shows the laminar flow velocity development for a Hartmann number M of zero. This is compared with the finite difference solution of Bodoia and Osterle.[8] Even though the core flow velocities (large y values) are somewhat in error, the nearwall velocities (small y values) follow the finite difference solution quite closely. Such behavior is also observed at a Hartmann number of 4, where the finite difference solution of Shohet et al[9] is applicable. Accuracy of the velocity profile near the wall is more important than elsewhere, because the wall stress and, hence, the friction coefficient must be calculated there.

Figure 2 illustrates the pressure drop development at a Hartmann number of 4 as compared with the results of Shohet et al.[9] All the curves in this figure correspond to one solution of Eq. (3). As can be seen, the accuracy is quite good. Good accuracy is also obtained at a Hartmann number of zero.

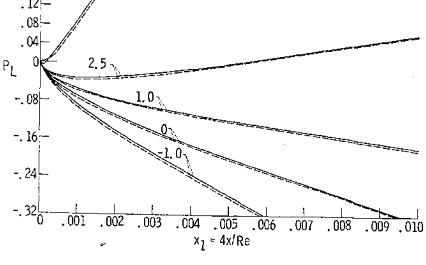

Fig. 2 Laminar flow pressure drop development for Hartmann number, $M = 4$.

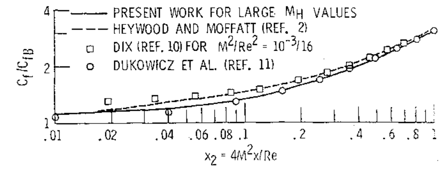

Fig. 3 Ratio of local friction coefficient to Blasius friction coefficient as a function of distance [$C_{fb} = 0.664(\mu/\rho UX)^{1/2}$].

Figure 3 is a comparison of the present work with the numerical flat plate results of Dix[10] and Dukowicz et al[11] and the momentum integral-Hartmann profile method of Heywood and Moffatt.[2] Here, the simpler Eq. (6) is used rather than (5) because $\epsilon \gg 1$ throughout the flow. The agreement is quite good, particularly with the results of Dukowicz et al.[11] These numerical results should be somewhat more accurate than those of Dix,[10] because a von Mises transformation was used to remove the leading edge singularity.

The momentum integral method of Heywood and Moffatt[2] is also seen to be accurate for predicting the friction coefficient along a flat plate. However, it should be remembered that theirs are numerical results, whereas the present calculations were made from simple analytical results obtained by using Eq. (6) in Eq. (7).

Concluding Remarks

1) It appears that, in applying the momentum integral approach to the entrance flow in an MHD channel, it is important to include viscous stresses in the core flow as well as in the boundary layer, which can be done by defining an edge stress.

2) The presence of an edge shear stress term in the integral equation of motion allows solutions to be obtained which are a) analytical, b) accurate both near to and far from the entrance, and c) which can be used with a variety of entrance conditions.

References

[1] Schwirian, R. E., "A New Momentum-Integral Method for Treating MHD and Simple Hydrodynamic Entrance Flows," AIAA Paper 69-724, San Francisco, Calif., 1969.

[2] Heywood, J. B. and Moffatt, W. C., "Validity of Integral Methods in MHD Boundary-Layer Analyses," *AIAA Journal*, Vol. 3, No. 8, Aug. 1965, pp. 1565–1567.

[3] Dhanak, A. M., "Heat Transfer in Magnetohydrodynamic Flow in an Entrance Section," paper 64-HT-30, Aug. 1964, American Society of Mechanical Engineers.

[4] Moffatt, W. C., "Analysis of MHD Channel Entrance Flows Using the Momentum Integral Method," *AIAA Journal*, Vol. 2, No. 8, Aug. 1964, pp. 1495–1497.

[5] Maciulaitis, A. and Loeffler, A. L., "A Theoretical Investigation of MHD Channel Entrance Flows," *AIAA Journal*, Vol. 2, No. 12, Dec. 1964, pp. 2100–2103.

[6] Tan, W. C., "Laminar MHD Channel Entrance Flows," *AIAA Journal*, Vol. 3, No. 7, July 1965, pp. 1369–1371.

[7] Hartmann, J., "Mercury Dynamics. I. Theory of the Laminar Flow of an Electrically Conductive Liquid in a Homogeneous Magnetic Field," *Kongelige Danske Videnskabernes Selskab Mathematisk-Fysiske Meddelelser*, Vol. 15, No. 6, 1937.

[8] Bodoia, J. R. and Osterle, J. F., "Finite Difference Analysis of Plane Poiseuille and Couette Flow Developments," *Applied Scientific Research*, Sec. A, Vol. 10, 1961, pp. 265–276.

[9] Shohet, J. L., Osterle, J. F., and Young, F. J., "Velocity and Temperature Profiles for Laminar Magnetohydrodynamic Flow in the Entrance Region of a Plane Channel," *The Physics of Fluids*, Vol. 5, No. 5, May 1962, pp. 545–549.

[10] Dix, D. M., "The Magnetohydrodynamic Flow Past a Non-conducting Flat Plate in the Presence of a Transverse Magnetic

Field," Ph.D. thesis, 1961, Massachusetts Institute of Technology, Cambridge, Mass.

[11] Dukowicz, J. K., Matthias, C. J., and de Leeuw, J. H., "The Flat-Plate Magnetohydrodynamic Boundary Layer in a Transverse Magnetic Field," *Canadian Aeronautics and Space Institute Transactions*, Vol. 1, No. 1, March 1968, pp. 45–51.

Unsymmetrical Bending of Shells of Revolution

J. J. BLECH*
Ford Motor Company, Dearborn, Mich.

BASED on the general first-order shell theory of Sanders, B. Budiansky and P. P. Radkowski[1] derived a set of four governing second-order differential equations. It has been pointed out by several authors[2–4] that for a computer analysis it is convenient to use as dependent variables those quantities which appear in the boundary conditions, thus reducing the shell field equations into a system of eight first-order differential equations. In such a formulation the computation of derivatives of wall properties is avoided. In case of the Sanders theory, using the same notation as in Ref. 1 a first-order system of equations is derived from the 17 field Eqs. (27–32) of Ref. 1 with the aid of Eqs. (5–7, 46, 49). This set of equations can be written in the matrix form

$$Z' = AZ + P \tag{1}$$

where the elements Z_i, P_i of the 8×1 column vectors Z, P, respectively, are given by

$$Z_1 = u_\xi, \quad Z_2 = u_\theta, \quad Z_3 = w, \quad Z_4 = \varphi_\xi, \quad Z_5 = t_\xi \qquad Z_6 = \hat{t}_{\xi\theta}, \quad Z_7 = \hat{f}_\xi, \quad Z_8 = m_\xi \tag{2a}$$

$$\begin{gathered} P_1 = -t_T/b, \quad P_2 = 0, \quad P_3 = 0, \quad P_4 = -m_T/d \\ P_5 = \gamma(1-\nu)t_T - p_\xi \\ P_6 = n/\rho(1-\nu)\,(t_T + \lambda^2\omega_\theta m_T) - p_\theta \\ P_7 = (1-\nu)\,(\omega_\theta t_T + \lambda^2 n^2/\rho^2 m_T) - p \\ P_8 = \gamma(1-\nu)m_T \end{gathered} \tag{2b}$$

and the elements A_{ij} of the 8×8 matrix A are as follows

$$A_{11} = A_{41} = -\nu\gamma \tag{3a}$$

$$A_{12} = -A_{66} = -\nu n/\rho \tag{3b}$$

$$A_{13} = -A_{76} = -\omega_\xi - \nu\omega_\theta \tag{3c}$$

$$A_{16} = 1/b \tag{3d}$$

$$A_{21} = -A_{57} = (n/\rho)[1 - (\lambda^2 d/bc)(3\omega_\theta - \omega_\xi)\omega_\theta] \tag{3e}$$

$$A_{22} = -A_{56} = -A_{78} = -\tfrac{1}{2}A_{67} = \gamma \tag{3f}$$

$$A_{23} = \gamma A_{24} = -A_{77} = -\lambda^2 A_{87} = (\lambda^2 d/bc)(n/\rho)(3\omega_\theta - \omega_\xi) \tag{3g}$$

$$A_{27} = (2/bc)(1-\nu) \tag{3h}$$

$$A_{31} = -A_{58} = \omega_\xi \tag{3i}$$

$$A_{34} = -1 \tag{3j}$$

$$A_{42} = -(1/\lambda^2)A_{65} = -(\nu n/\rho)\omega_\theta \tag{3k}$$

$$A_{43} = -(1/\lambda^2)A_{75} = -\nu n^2/\rho^2 \tag{3l}$$

$$A_{45} = 1/d \tag{3m}$$

$$A_{51} = b(1-\nu^2)\left[\gamma^2 + \frac{2}{(1+\nu)c}\frac{\lambda^2 d}{b}\frac{n^2}{\rho^2}\omega_\theta^2\right] \tag{3n}$$

$$A_{52} = A_{61} = b(1-\nu^2)(n/\rho)\gamma \tag{3o}$$

$$A_{53} = A_{71} = b(1-\nu^2)\omega_\theta\gamma\left[1 - \frac{2}{(1+\nu)c}\frac{\lambda^2 d}{b}\frac{n^2}{\rho^2}\right] \tag{3p}$$

$$A_{54} = \lambda^2 A_{81} = \lambda^2 d(1-\nu^2)[2/(1+\nu)c](n^2/\rho^2)\omega_\theta \tag{3q}$$

$$A_{62} = b(1-\nu^2)(n^2/\rho^2)[1 + (\lambda^2 d/b)\omega_\theta^2] \tag{3r}$$

$$A_{64} = \lambda^2 A_{82} = \lambda^2 d(1-\nu^2)(n/\rho)\gamma\omega_\theta \tag{3s}$$

$$A_{73} = b(1-\nu^2)\left\{\omega_\theta^2 + \frac{\lambda^2 d}{b}\frac{n^2}{\rho^2}\left[\frac{n^2}{\rho^2} + \frac{2}{(1+\nu)c}\gamma^2\right]\right\} \tag{3t}$$

$$A_{74} = \lambda^2 A_{83} = \lambda^2 d(1-\nu^2)\frac{n^2}{\rho^2}\gamma\left[1 + \frac{2}{(1+\nu)c}\right] \tag{3u}$$

$$A_{84} = d(1-\nu^2)[\gamma^2 + \{2/(1+\nu)c\}n^2/\rho^2] \tag{3v}$$

$$A_{85} = -(1-\nu)\gamma \tag{3w}$$

$$A_{88} = 1/\lambda^2 \tag{3x}$$

where

$$c = 1 + (1/4)(\lambda^2 d/b)(3\omega_\theta - \omega_\xi)^2 \tag{4}$$

and all the other A_{ij}'s are equal to zero.

Equation (80) of Ref. 1 is replaced by

$$\sigma_\xi^{(n)} = \frac{\sigma_0}{(1-\nu^2)}\left(\frac{1}{b}t_\xi + \frac{1}{d}\frac{\zeta}{a}m_\xi\right) + \frac{t_T}{b} + \frac{\zeta}{a}\frac{m_T}{d} - \frac{E\alpha T^{(n)}}{(1-\nu)} \tag{5a}$$

$$\sigma_\theta^{(n)} = \sigma_0\left[\gamma u_\xi + \frac{n}{\rho}\left(1 + \omega_\theta\frac{\zeta}{a}\right)u_\theta + \left(\omega_\theta + \frac{\zeta}{a}\frac{n^2}{\rho^2}\right)\times w + \gamma\frac{\zeta}{a}\varphi_\xi + \frac{\nu}{(1-\nu^2)}\left(\frac{1}{b}t_\xi + \frac{1}{d}\frac{\zeta}{a}m_\xi\right)\right] + \nu\frac{t_T}{b} + \nu\frac{\zeta}{a}\frac{m_T}{d} - \frac{E\alpha T^{(n)}}{(1-\nu)} \tag{5b}$$

$$\sigma_{\xi\theta}^{(n)} = \frac{\sigma_0}{(1+\nu)}\left\{\left[cA_{24} - \frac{n}{\rho}\frac{\zeta}{a}\right](-\omega_\theta u_\xi + \gamma w + \varphi_\xi) + \frac{1}{bc(1-\nu)}\left[1 + (3\omega_\theta - \omega_\xi)\frac{\zeta}{a}\right]\hat{t}_{\xi\theta}\right\} \tag{5c}$$

By partitioning the column vector Z into two 4×1 column vectors $y = (u_\xi, u_\theta, w, \varphi_\xi)$ and $z = (t_\xi, \hat{t}_{\xi\theta}, \hat{f}_\xi, m_\xi)$, the branch point transition relations (B1), (B2) of Ref. 1 are simplified to

$$y^{\mathrm{III}} = \psi^{\mathrm{II}}y^{\mathrm{II}} = \psi^{\mathrm{I}}y^{\mathrm{I}} \tag{6a}$$

$$z^{\mathrm{III}} = \psi^{\mathrm{II}}z^{\mathrm{II}} + \psi^{\mathrm{I}}z^{\mathrm{I}} \tag{6b}$$

where the matrix ψ is given by Eq. (57) of Ref. 1.

The boundary conditions and discontinuity condition equations that are used in the present formulation are similar to Eqs. (47, 55, and 56) of Ref. 1, respectively.

References

[1] Budiansky, B. and Radkowski, P. P., "Numerical Analysis of Unsymmetrical Bending of Shells of Revolution," *AIAA Journal*, Vol. 1, No. 8, Aug. 1963, pp. 1833–1842.

[2] Cohen, G. A., "Computer Analysis of Asymmetrical Deformation of Orthotropic Shells of Revolution," *AIAA Journal*, Vol. 2, No. 5, May 1964, pp. 932–934.

[3] Goldberg, J. E., "Computer Analysis of Shells," 70th Anniversary Symposium on the Theory of Shells, Univ. of Houston, April 1966.

[4] Kalnins, A., "Analysis of Shells of Revolution Subjected to Symmetrical and Nonsymmetrical Loads," *Journal of Applied Mechanics*, Vol. 31, Sept. 1964, pp. 467–476.

Received September 15, 1969.

* Turbine Research Specialist.